COMPDYN 2015
5th ECCOMAS Thematic Conference on
Computational Methods in Structural Dynamics and Earthquake Engineering
M. Papadrakakis, V. Papadopoulos, V. Plevris (eds.)
Crete Island, Greece, 25–27 May 2015

DE^3: YET ANOTHER HIGH-ORDER INTEGRATION SCHEME FOR LINEAR STRUCTURAL DYNAMICS

Alexandre Depouhon[1,2], Emmanuel Detournay[2], and Vincent Denoël[1]

[1]Structural and Stochastic Dynamics, Université de Liège
1, rue des Chevreuils, 4000 Liège, Belgium
e-mail: v.denoel@ulg.ac.be

[2] Civil, Environmental and Geo- Engineering Department, University of Minnesota
500, Pillsbury Drive S.E., 55455, MN, Minneapolis, USA
e-mail: {depou002, detou001}@umn.edu

Keywords: Structural dynamics, Integration scheme, High-order accuracy, Unconditional stability

Abstract. *In this paper, we present the* DE^3 *integration scheme. This unconditionally stable scheme is dedicated to the numerical integration of linear structural dynamics problems and offers a simple and easy to use high-order alternative to the second-order accurate ones that are usually employed. Its symmetric formulation makes it an interesting candidate to simulate large-scale problems. In addition, the scheme offers the possibility to control the introduced numerical damping via a single algorithmic parameter, which is very convenient for the filtering of the spurious oscillations that can arise from large stiffness contrasts in certain models. The properties of high-order accuracy and numerical damping are illustrated by way of a demonstrative example.*

1 INTRODUCTION

Since Newmark's landmark paper [1], a vast number of integration schemes have been developed to advance in time the canonical equation of motion of linear structural dynamics

$$\mathbf{M}\ddot{\mathbf{u}}(t) + \mathbf{C}\dot{\mathbf{u}}(t) + \mathbf{K}\mathbf{u}(t) = \mathbf{f}(t). \tag{1}$$

These are typically derived from the mathematical treatment of the equation of motion and continuity assumptions of the field to be discretized, *e.g.*, Taylor expansion, finite element approaches based on weak formulations, or finite difference approximations. For linear problems, what matters, though, are the stability and accuracy properties of the derived schemes, their structure-preserving nature (energy conservation for instance), if any, as well as their intrinsic computational cost.

The DE^3 scheme [2] belongs to the class of two-level one-step implicit integration schemes enjoying unconditional stability. It is a reformulation of the scheme proposed by Bottasso and Trainelli [3] by condensation of the original scheme internal variables. As such, it exhibits the same properties. Namely, it preserves the linear momentum of the mechanical system and offers control on the numerical dissipation of mechanical energy, in the high-frequency range, via a single parameter. It is fourth-order accurate when used in its conservative setting; the accuracy drops to third order when numerical damping is present, however. This makes it an ideal candidate for structural dynamics simulations [4] or, even, wave propagation ones in combination with the finite element method [5], as the numerical dissipation enables the control of high-frequency Gibbs oscillations.

The focus of this contribution is set on the derivation of the scheme and the illustration of its superior features by application to an example problem of structural dynamics.

2 THE DE^3 SCHEME

Related to the time discontinuous Galerkin method [6] that is built on the assumption of possible discontinuities of the underlying integrated field, the method proposed by Bottasso and Trainelli [3] is similarly formulated in terms of the left and right limits of the field variables at the time nodes. Assuming equation (1) to hold with constant symmetric stiffness, damping and mass matrices under the typical positiveness assumptions ($\mathbf{K}, \mathbf{C} \geq 0$ and $\mathbf{M} > 0$), the integration scheme they proposed reads

$$\begin{aligned}
&\begin{pmatrix} \frac{1}{2}\mathbf{K} & \frac{1}{h}\mathbf{M} + \frac{1}{2}\mathbf{C} & \frac{1}{2}\mathbf{K} & \frac{1}{2}\mathbf{C} \\ \mathbf{I} & -\frac{h}{2}\mathbf{I} & \mathbf{0} & -\frac{h}{2}\mathbf{I} \\ \mathbf{0} & \frac{h}{6}\mathbf{I} & \mathbf{I} & -\beta\frac{h}{6}\mathbf{I} \\ -\frac{1}{6}\mathbf{K} & -\frac{1}{6}\mathbf{C} & \frac{\beta}{6}\mathbf{K} & \frac{1}{h}\mathbf{M} + \frac{\beta}{6}\mathbf{C} \end{pmatrix} \begin{pmatrix} \mathbf{u}_{n+1} \\ \mathbf{v}_{n+1} \\ \mathbf{u}_{n^+} \\ \mathbf{v}_{n^+} \end{pmatrix} \\
&\qquad = \begin{pmatrix} \mathbf{0} & \frac{1}{h}\mathbf{M} \\ \mathbf{I} & \mathbf{0} \\ \mathbf{I} & (1-\beta)\frac{h}{6}\mathbf{I} \\ \frac{\beta-1}{6}\mathbf{K} & \frac{1}{h}\mathbf{M} + \frac{\beta-1}{6}\mathbf{C} \end{pmatrix} \begin{pmatrix} \mathbf{u}_n \\ \mathbf{v}_n \end{pmatrix} + \begin{pmatrix} \frac{1}{h}\mathbf{I}_1 \\ \mathbf{0} \\ \mathbf{0} \\ \frac{2}{h^2}\left(t_{n+1/2}\mathbf{I}_1 - \mathbf{I}_2\right) \end{pmatrix},
\end{aligned} \tag{2}$$

where

$$\mathbf{I}_1 = \int_{t_n}^{t_{n+1}} \mathbf{f}(t)\,\mathrm{d}t, \qquad \mathbf{I}_2 = \int_{t_n}^{t_{n+1}} t\mathbf{f}(t)\,\mathrm{d}t \tag{3}$$

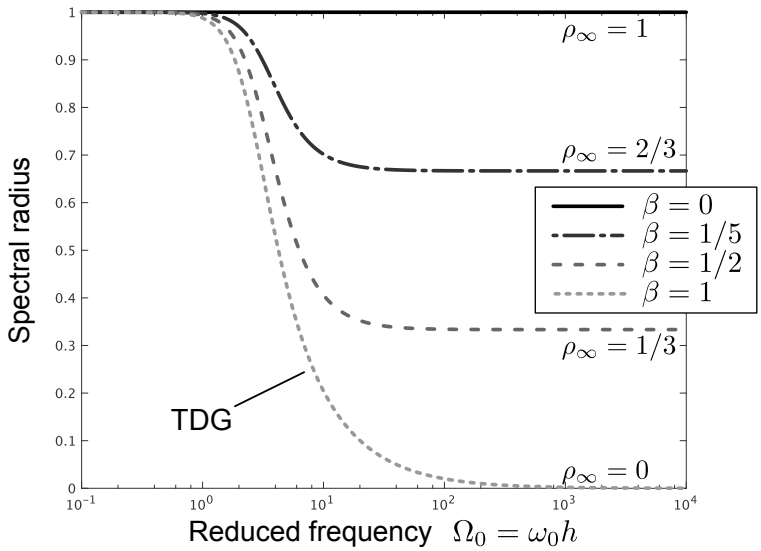

Figure 1: The algorithmic parameter β enables the control of the numerical dissipation introduced by the scheme. For $\beta = 0$, the integration scheme preserves the mechanical energy whereas it numerically dissipates some for $\beta \in (0, 1]$. The time discontinuous Galerkin scheme (TDG) is recovered for $\beta = 1$. After [2].

denote the first- and second-order non-centered time moments of the external forces over the timestep, and $\mathbf{u}, \mathbf{v}$ represent the displacement and velocity fields. The indices refer to the time argument of these fields; the syntax is equivalent to

$$\mathbf{x}_n = \lim_{\epsilon \to 0^-} \mathbf{x}(t_n + \epsilon), \qquad \mathbf{x}_{n^+} = \lim_{\epsilon \to 0^+} \mathbf{x}(t_n + \epsilon). \tag{4}$$

Parameter $\beta \in [0, 1]$ is an algorithmic parameter that controls the numerical dissipation introduced by the scheme. It is related to the spectral radius of the integration scheme amplification matrix at infinite frequency ρ_∞ through the following expression

$$\beta = \frac{1 - \rho_\infty}{1 + \rho_\infty} \quad \leftrightarrow \quad \rho_\infty = \frac{1 - \beta}{1 + \beta}. \tag{5}$$

For $\beta = 0$, the scheme is conservative, in the sense that it preserves the mechanical energy of the system , whereas for $\beta \in (0, 1]$ it is numerically dissipative. In the particular case of $\beta = 1$, the time discontinuous Galerkin method is recovered. This configuration is spectrally annihilating, as can be seen in Figure 1 that shows the evolution of the spectral radius of the scheme in the case of the undamped/unforced single degree of freedom spring/mass oscillator. Furthermore, the study of the balance of mechanical energy over a timestep shows that the scheme is conservative when $\beta = 0$ and dissipative otherwise.

As the right-limit values $\mathbf{u}_{n^+}, \mathbf{v}_{n^+}$ only appear on left-hand side of (1), they can be considered as internal variables to the integration scheme and can be eliminated via static condensation. A double application of the block inversion formula [7] enables the reduction of the four-level formulation (2) to an equivalent two-level formulation based on the displacement and velocity fields only. Completing all the algebra—see [2] for the details—the DE^3 scheme is obtained

$$\mathbf{H}_0 \mathbf{x}_{n+1} = \mathbf{H}_1 \mathbf{x}_n + \boldsymbol{\ell}_n^{n+1}, \tag{6}$$

with

$$
\begin{aligned}
\mathbf{x}_n &= \begin{pmatrix} \mathbf{u}_n \\ \mathbf{v}_n \end{pmatrix}, \\
\mathbf{H}_0 &= \begin{pmatrix} \mathbf{C} + \left(\frac{1}{2} + \frac{\beta}{6}\right) h\mathbf{K} & \mathbf{M} - \left(\frac{1}{12} + \frac{\beta}{12}\right) h^2\mathbf{K} \\ \mathbf{M} - \left(\frac{1}{12} + \frac{\beta}{12}\right) h^2\mathbf{K} & -\left(\frac{1}{2} + \frac{\beta}{6}\right) h\mathbf{M} - \left(\frac{1}{12} + \frac{\beta}{12}\right) h^2\mathbf{C} \end{pmatrix}, \\
\mathbf{H}_1 &= \begin{pmatrix} \mathbf{C} - \left(\frac{1}{2} - \frac{\beta}{6}\right) h\mathbf{K} & \mathbf{M} - \left(\frac{1}{12} - \frac{\beta}{12}\right) h^2\mathbf{K} \\ \mathbf{M} - \left(\frac{1}{12} - \frac{\beta}{12}\right) h^2\mathbf{K} & \left(\frac{1}{2} - \frac{\beta}{6}\right) h\mathbf{M} - \left(\frac{1}{12} - \frac{\beta}{12}\right) h^2\mathbf{C} \end{pmatrix}, \\
\boldsymbol{\ell}_n^{n+1} &= \begin{pmatrix} \mathbf{I}_1 \\ \left(t_{n+1/2} - \frac{\beta}{6}h\right) \mathbf{I}_1 - \mathbf{I}_2 \end{pmatrix}.
\end{aligned}
\tag{7}
$$

As the algebraic manipulations leading to DE^3 scheme do not alter the structure of the scheme (2), it enjoys the same properties. Namely, the algorithmic parameter β controls the spectral radius of the amplification matrix at infinite frequency, in accordance with (5), and therefore the amount of numerical dissipation introduced during integration. It also plays a role on the accuracy of the scheme which can be demonstrated to be fourth-order for $\beta = 0$ (numerically conservative scheme) or third-order for $\beta \in (0, 1]$ (numerically dissipative scheme). Note that high-order accuracy requires that the integrals $\mathbf{I}_1$ and $\mathbf{I}_2$ be computed with at least third degree exactness, as is for instance offered by the Simpson-Cavalieri rule [8]. In such case, after completing the algebra relative to the definition of the error metrics introduced in [2], it can be shown that the local truncation errors for the free and forced responses are asymptotic to

$$L_{\text{free}} \sim \beta\, f_{\text{free}}(\omega_0, \zeta) h^3 + g_{\text{free}}(\omega_0, \zeta, \beta) h^4, \tag{8}$$

$$L_{\text{forced}} \sim \beta\, f_{\text{forced}}(\omega_0, \zeta) h^3 + g_{\text{forced}}(\omega_0, \zeta, \beta) h^4, \tag{9}$$

for $h \ll \omega_0^{-1}$, with functions $g_{\text{free}}(\omega_0, \zeta, \beta)$ and $g_{\text{forced}}(\omega_0, \zeta, \beta)$ not vanishing when $\beta = 0$, and ω_0, ζ denoting the natural frequency and damping coefficient of a single degree of freedom spring/dashpot/mass oscillator periodically excited. Similarly to the original formulation, the two-level one is unconditionally stable.

The two-level formulation of the DE^3 scheme offers a couple of advantages over the original four-level formulation proposed by Bottasso and Trainelli. In particular, it is of lower size, as the update equations no longer involve internal states, and it is symmetric, which is favorable to reducing the storage size of matrices $\mathbf{H}_0, \mathbf{H}_1$ when dealing with large models. Also, in comparison to other integration schemes that can employ multiple algorithmic parameters, the control of numerical dissipation is achieved via a single algorithmic parameter, which makes the integration scheme simple to use.

It is actually found that the DE^3 scheme is very similar to the one proposed by Krenk [9], which was derived from the equation of motion via a weak formulation. A significant difference between the DE^3 scheme and that proposed by Krenk concerns the handling of the contributions of the damping and the external forcing terms, which allow the DE^3 scheme to retain its fourth- (and third-) order accuracy in the conservative (resp. dissipative) setting when integrating forced and/or damped structural models, contrary to Krenk's formulation.

3 DEMONSTRATIVE EXAMPLE

To illustrate the performance of the scheme, we consider the two degree-of-freedom oscillator depicted in Figure 2. This model has a single parameter Ω that is representative of the stiffness contrast that could be encountered in finite element models; in the extreme case $\Omega \gg 1$, the stiff element can be interpreted as a penalty used to enforce a constraint. For this specific

model, the $\Omega \gg 1$ case corresponds to imposing a rigid link between degree-of-freedom 1 and the boundary with imposed displacement.

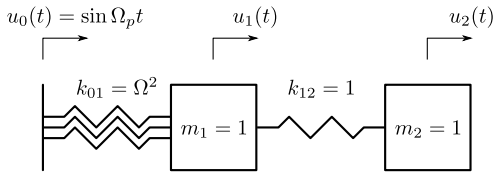

Figure 2: Soft/stiff linear oscillator. External forcing is applied by controlling the displacement $u_0(t)$.

In the first part of this example, we compare the accuracy achieved by the DE^3 scheme to two other well-known integration schemes, namely the ones proposed by Newmark [1] and Bathe [10]. In the second part, we illustrate the utility of numerical damping in structural simulations and, in particular, the property of spectral annihilation that the DE^3 scheme enjoys when used in its most dissipative setting. In both parts, the forcing frequency is set to $\Omega_p = 1.2$.

To quantify the error resulting from the numerical integration of the equations of motion, we use the energy-based metric introduced in [2]

$$\mathcal{E}(t) := \frac{1}{\sqrt{2}} \sqrt{(\mathbf{u}(t) - \underline{\mathbf{u}}(t))^T \mathbf{K} (\mathbf{u}(t) - \underline{\mathbf{u}}(t)) + (\mathbf{v}(t) - \underline{\mathbf{v}}(t))^T \mathbf{M} (\mathbf{v}(t) - \underline{\mathbf{v}}(t))}, \qquad (10)$$

where the reference trajectory, denoted by an underlined variable, is calculated using modal superposition [11]. For a proper assessment of the error, the system oscillations must be sufficiently resolved. In other words, the timestep must be small enough to ensure a sufficient number of computed points per period of the highest frequency signals. It is easily shown that this frequency is set by the largest eigenfrequency of the model. For the soft/stiff oscillator, the two eigenfrequencies read

$$\Omega_1 = \frac{\sqrt{4 + 2\Omega^2 - 2\sqrt{4 + \Omega^4}}}{2}, \qquad \Omega_2 = \frac{\sqrt{4 + 2\Omega^2 + 2\sqrt{4 + \Omega^4}}}{2}, \qquad (11)$$

and follow the evolution shown in Figure 3 when parameter Ω is varied. One eigenvalue is always approximately equal to Ω and the other tends to $\sqrt{2}$ or 1 if $\Omega < 1$ or $\Omega > 1$. In the absence of damping, the oscillatory response of the model comprises three frequency component: $\Omega_1, \Omega_2, \Omega_p$. Setting $\Omega = 100$, we have $\Omega_2 > \Omega_p > \Omega_1$ and the resolution constraint is set by $\Omega_2 \simeq 100$. Twelve points per period lead to a timestep requirement of $h \leq 5 \cdot 10^{-3}$.

The evolution of the error $\mathcal{E}(10)$ with the timestep $h \in [5 \cdot 10^{-5}, 5 \cdot 10^{-3}]$ is shown in Figure 4. The high-order nature of the DE^3 scheme is well established over the other considered methods. By order of increasing accuracy, we observe the following ranking: Newmark's scheme ($(\beta, \gamma) = (1/4, 1/2)$) is less accurate than Bathe's method [10]—both are second-order methods—than the DE^3 scheme that is third-order accurate in its dissipative setting ($\rho_\infty = 0.5$) and fourth-order accurate in its conservative setting ($\rho_\infty = 1$). It is observed that the requirement of twelve points per lowest period is not sufficient to ensure proper accuracy with the second-order methods whereas it does for the DE^3 scheme.

Besides offering high-order accuracy integration, the DE^3 scheme can also be tuned to damp Gibbs oscillations that can arise from the finite resolution of the finite elements typically used in structural dynamics. This can be illustrated by setting $\Omega \gg 1$ in the soft/stiff model and

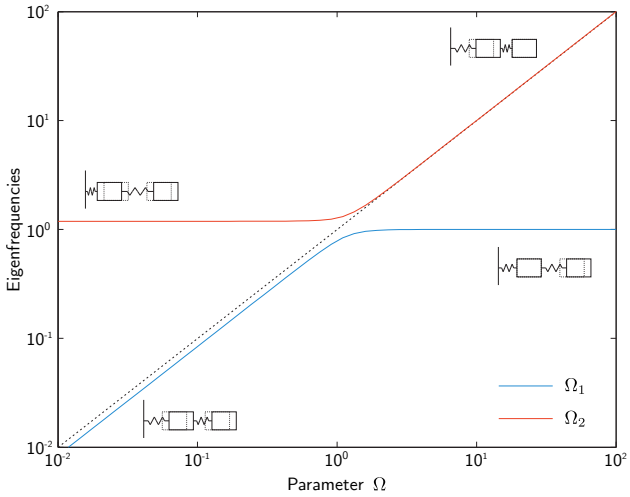

Figure 3: Evolution of the eigenfrequencies with parameter Ω.

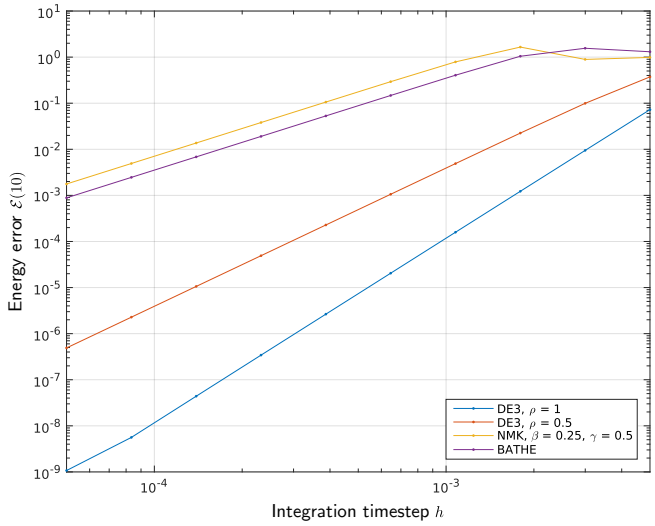

Figure 4: Comparison of the error introduced by the numerical integration procedure for several schemes. The slopes of the lines give the order of accuracy of the schemes.

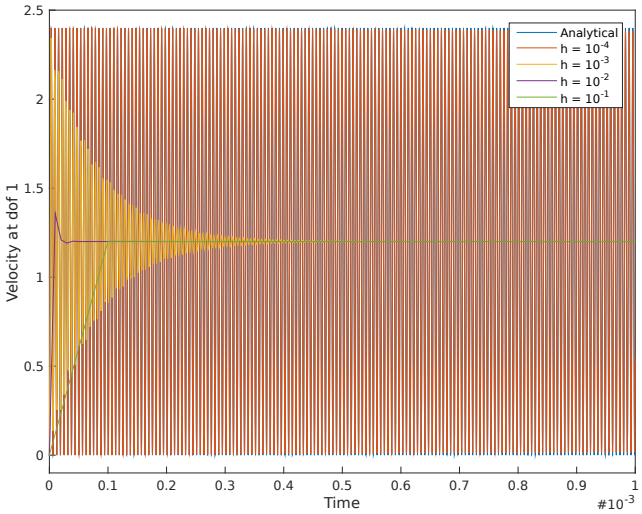

Figure 5: Taming of spurious oscillations via the proper adjustment of the numerical damping introduced by the DE^3 scheme.

by interpreting the high-frequency oscillations at $\Omega_2 \sim \Omega + (2\Omega)^{-1} + O(\Omega^{-3})$ to be spurious ones. Proper filtering should then be achieved to ensure that they do not contaminate the lower frequency components of the model response so that its dynamics is well resolved.

From Figure 1, we see that high-frequency oscillations are very quickly damped by the integration scheme if $\rho_\infty = 0$ (most dissipative configuration) and the frequency-reduced timestep is above 10^2, as the magnitude of the spectral radius of the amplification matrix is indicative of the scaling of the amplitude of harmonic oscillations over a single integration increment. We can thus deduce that spurious oscillations will be fast rejected by the integration scheme provided

$$h > h^* = \frac{10^3}{\Omega_2} \simeq \frac{10^3}{\Omega}. \tag{12}$$

Setting $\Omega = 10^6$ and keeping $\Omega_p = 1.2$, so that there is a timescale separation between the slow dynamics we are interested in and the spurious dynamics, the above criterion reduces to $h > h^* \simeq 10^{-3}$. Figure 5 illustrates the effect of numerical damping on the spurious oscillations, by varying the integration timestep while keeping the numerical setting to $\rho_\infty = 0$. Reducing the timestep is equivalent to moving leftwards along the x-axis of Figure 1 and, thus, the larger the timestep, the more damping is introduced with respect to the frequency set by $\Omega_2 \simeq \Omega$. As expected, the high-frequency oscillations are more quickly damped for large timesteps than for small ones. In fact, they are even annihilated in one increment for $h = 10^{-1}$, whence the name of the spectral annihilation property. The DE^3 scheme thus not only offers high accuracy but also control on the numerical dissipation introduced in the simulations, making it an interesting candidate for structural dynamics computations.

4 CONCLUSION

The DE^3 scheme positions itself as a novel and unconditionally stable high-order alternative to the second-order schemes commonly used in structural dynamics. Its symmetric formulation, combined to the possibility it offers to control numerical damping via a single parameter, make it an ideal algorithmic solution for the simulation of large-scale structural dynamics problems.

Indeed, advantage can be taken from its symmetric nature on the solver side while the controlled numerical damping can be used to tame spurious oscillations that typically arise in problems showing a broad spectrum of eigenfrequencies, with the higher ones being associated with numerical rather than physical eigenmodes.

In this paper, those properties are established and demonstrated by way of an example. In particular, an error analysis shows its superiority on other well-know schemes and the control of numerical damping to remove spurious oscillations is illustrated as well.

REFERENCES

[1] N.M. Newmark. A method of computation for structural dynamics. *Journal of Engineering Mechanics, ASCE*, 85(EM3):67–94, 1959.

[2] A. Depouhon, E. Detournay, and V. Denoël. Accuracy of one-step integration schemes for damped/forced linear structural dynamics. *International Journal for Numerical Methods in Engineering*, 99(5):333–353, August 2014.

[3] C.L. Bottasso and L. Trainelli. An Attempt at the Classification of Energy Decaying Schemes for Structural and Multibody Dynamics. *Multibody System Dynamics*, 12:173–185, 2004.

[4] A. Depouhon, E. Detournay, and V. Denoël. Event-driven integration of linear structural dynamics models under unilateral elastic constraints. *Computer Methods in Applied Mechanics and Engineering*, 276(0):312–340, July 2014.

[5] A. Depouhon, , V. Denoël, and E. Detournay. Numerical simulation of percussive drilling. *International Journal for Numerical and Analytical Methods in Geomechanics*, (Online) 2015.

[6] X.D. Li and N.-E. Wiberg. Structural Dynamic Analysis by a Time-Discontinuous Galerkin Finite Element Method. *International Journal for Numerical Methods in Engineering*, 39(12):2131–2152, 1996.

[7] L. Guttman. Enlargement Methods for Computing the Inverse Matrix. *The Annals of Mathematical Statistics*, 17:336–343, 1946.

[8] A. Quarteroni, R. Sacco, and F. Saleri. *Numerical Mathematics*. Texts in Applied Mathematics. Springer-Verlag New York, Inc., 2010.

[9] S. Krenk. State-space time integration with energy control and fourth-order accuracy for linear dynamic systems. *International Journal for Numerical Methods in Engineering*, 65:595–619, January 2006.

[10] K.-J. Bathe and G. Noh. Insight into an implicit time integration scheme for structural dynamics. *Computers and Structures*, 98–99:1–6, 2012.

[11] M. Géradin and D. Rixen. *Mechanical Vibrations: Theory and Application to Structural Dynamics*. Wiley, 1997.